Influence of the strong metal support interaction effect (SMSI) of Pt/TiO2 and Pd/TiO2 systems in the photocatalytic biohydrogen production from glucose solution

Juan C. Colmenares (a), Agnieszka Magdziarz (a), Maria A. Aramendia (b), Alberto Marinas (b), José M. Marinas (b), Francisco J. Urbano (b), José A. Navio (c)

(a) Institute of Physical Chemistry PAS, Kasprzaka 44/52, 01–224 Warsaw, Poland

(b) Organic Chemistry Department, University of Córdoba, Campus de Rabanales, Marie Curie Building, E-14014 Córdoba, Spain

(c) Instituto de Ciencia de Materiales de Sevilla, Centro Mixto Universidad de Sevilla-CSIC, Americo Vespucio s/n, E-41092 Sevilla, Spain

Abstract

Two different catalysts consisting of Pt/TiO2 and Pd/TiO2 were submitted to diverse oxidative and reductive calcination treatments and tested for photocatalytic reforming of glucose water solution (as a model of biomass component) in H2 production. Oxidation and reduction at 850 °C resulted in better photocatalysts for hydrogen production than Degussa P-25 and the ones prepared at 500 °C, despite the fact that the former consisted in very low surface area (6–8 m2/g) rutile titania specimens. The platinum-containing systems prepared at 850 °C give the most effective catalysts. XPS characterization of the systems showed that thermal treatment at 850 °C resulted in electron transfer from titania to metal particles through the so-called strong metal-support interaction (SMSI) effect. Furthermore, the greater the SMSI effect, the better the catalytic performance. Improvement in photocatalytic behavior is explained in terms of avoidance of electron–hole recombination through the electron transfer from titania to metal particles.

Keywords

Photocatalytic biomass reforming; H2 production; Water purification; Glucose; SMSI effect in photocatalysis

1. Introduction

Hydrogen production by solar light offers a promising method for the photochemical conversion and storage of solar energy.

Biomass sources could be utilized for the sustainable production of hydrogen [1]. A number of processes have been developed for this purpose (e.g., steam gasification [2], fast pyrolysis [3] and [4], and supercritical conversion [5] and [6]). However, these processes require harsh reaction conditions including high temperatures and/or pressures and consequently imply high costs. Compared to these energy intensive thermochemical processes, photocatalytic reforming may be a good approach as this process can be driven by sunlight and performed at room temperature. Producing hydrogen by photocatalytic reforming of renewable biomass

1

may also be more practical and viable than that of photocatalytic water splitting due to its potentially higher efficiency. Water-splitting processes are relatively low efficient as limited by the recombination reactions between photogenerated electrons and holes [7].

Food industry gives a huge amount of solid and liquid wastes (2nd generation biomass) which have to be valorizated. These non-toxic wastes become very harmful for natural environment if their concentration in water exceeds certain level. The sewage from food industry contains first of all water-soluble carbohydrates, the main ingredient of plants and plant food (e.g. glucose). Until now the sewage from food industry are purified using mainly biological methods. Photocatalytic decomposition of pollutants from food industry and photocatalytic production of clean hydrogen fuel can take place simultaneously when the pollutants act as electron donors (e.g. glucose). Using pollutants as electron donors shows the promise of the integration of pollutant decomposition and hydrogen production.

It is considered that the low efficiency for hydrogen production of semiconductor already with appropriate band gap is due to the following reasons: 1. quick electron/hole recombination in the bulk or on the surface of semiconductor particles [8], 2. quick back reaction of oxygen and hydrogen to form water on the surface of catalyst. There are also some other factors affecting photoefficiency such as the surface, crystallographic, and porosity properties of the semiconductor (e.g. TiO2 anatase/rutile/brookite). One of the methods to overcome such problems is the addition of small quantities of noble metals which can suppress to some extent the charge recombination by forming a Schottky barrier [9]. Moreover, VIII group metals supported on reducible supports present the so-called strong metal-support interaction (SMSI) effect when reduced at high temperatures as reported originally by Tauster et al. [10]. The SMSI effect in photocatalysis is not very well investigated, especially in the context of the reaction presented in this research work. Some studies have been shown the SMSI effect could help in the decrease of electron/hole recombination in semiconductors photocatalysis [11] and [12]. The aim of this work is to present the original results on the study of SMSI effect of Pd- and Pt-TiO2 photocatalysts on hydrogen production from a glucose aqueous solution. To the best of our knowledge, no reports on the effects of high-thermal redox treatment of metal-containing titania systems on the photocatalytic hydrogen production from a glucose aqueous solution can be found elsewhere.

2. Experiments

2.1. Photocatalysts preparation

The synthesis of the untreated platinum or palladium-containing titania systems was described in our previous work [13]. Fig. 1 summarizes the synthetic methodology applied to obtain the catalysts. Firstly, 0.25 mmol of titanium tetraisopropoxide (TTIP) was added dropwise to a beaker containing 270 mL of a isopropanol:water (10:1, v/v) mixture, under mechanical stirring at 0–5 °C; pH was then reduced to 2.5 with 60% HNO3 and sol samples were left under vigorous stirring, at 0–5 °C for 3 h. Subsequently, pH was increased up to 9 with 5 N NH4OH to form the gel which was submitted to ageing under ultrasonic irradiation (Ultrasonic Homogenizer 4710 Series, Cole-Palmer Instrument Co. 300 W, 20 kHz) during 10 h. The resulting gels were filtered under vacuum and washed with an aqueous solution of NH4OH at pH 9. They were then dried at 110 °C for 24 h, ground and sifted to a fine powder (particle

diameter < 0.149 mm). In the case of metal-containing systems, the acetylacetonate dissolved in 110 mL of isopropanol:water mixture (10:1, v/v) was added dropwise simultaneously to the addition of TTIP, as shown in Fig. 1. Finally, xerogels were calcined at 500 (6 h) and 850 °C (1 h) either in 10%H2/Ar (40 mL/min) or in synthetic air (30 mL/min) thus yielding the systems labeled as Pt-500-H, Pt-850-H, Pt-500-Air, Pt-850-Air and Pd-500-H, Pd-850-H, Pd-500-Air, Pd-850-Air, respectively.

2.2. Photocatalytic tests

All catalytic tests were performed in a Pyrex cylindrical double-walled immersion well reactor (reactor total volume 450 cm3) under Ar. Irradiation of the reaction solutions was carried out by using a medium pressure 125 W Hg lamp (λmax = 365 nm). Water used for cooling was thermostated at 30 °C. Solutions of pure glucose (500 ppm) were prepared in Milli-Q water. Experiments were carried out from 150 mL of the mother solution and 1 g/L of catalyst concentration was used. Experiments were done at room temperature and bubbling through the suspension pure Ar (40 mL/min). The amount of H2 evolved was determined by an on-line gas chromatograph (HP 5890 series II GC, Carboxen 1006 PLOT column, 30 m × 0.53 mm, TCD, Ar carrier). Glucose disappearance was monitored by HPLC (Waters Instrument with RI detector and XBridge™ Amide 3.5 µm 4.6 × 150 mm column. Mobile phase was a mixture of acetonitrile:H2O = 85:15 (v/v) with a flow rate of 0.8 mL/min and injection volume of 10 µL). For the sake of comparison, catalytic performance of Degussa P25 has also been included.

2.3. Photocatalysts characterization

The textural properties of solids were determined from N2 adsorption–desorption isotherms at liquid nitrogen temperature by using a Micromeritics ASAP 2010 instrument. Surface areas were calculated by the BET method. Prior to measurements, all samples were degassed at 110 °C to 0.1 Pa.

X-ray analysis of solids was carried out using a Siemens D-5000 diffractometer provided with an automatic control and data acquisition system (DACO-MP). The patterns were run with nickel-filtered copper radiation (λ = 1.5406 Å) at 40 kV and 30 mA; the diffraction angle 2θ was scanned at a rate of 2° min− 1. The average crystallite size of anatase and rutile was determined according to the Scherrer equation using the full-width at half-maximum of the peak corresponding to 101 and 110 reflections, respectively, and taking into account the instrument broadening.

TEM images were recorded in a JEOL JEM 2010 microscope operating at an accelerating voltage of 200 kV. Samples were previously embedded in an epoxy resin. Sections with a thickness of 40 nm were finally obtained with an ultramicrotome and mounted on 3-mm holey carbon copper grids.

XPS data were recorded on 4 mm × 4 mm pellets, 0.5 mm thick, prepared by slightly pressing the powdered materials which were outgassed in the prechamber of the instrument at 150 °C up to a pressure ≤ 2 × 10− 8 Torr to remove chemisorbed volatile species from their surfaces. The Leibold–Heraeus LHS10 spectrometer main chamber, working at a pressure ≤ 2 × 10− 9 Torr, was equipped with an EA-200 MCD hemispherical electron analyzer with a dual X-ray

source working with Al Ka (hy = 1486.6 eV) at 120 W, 30 mA using C(1 s) as energy reference (284.6 eV).

3. Results and discussion

Results obtained for hydrogen generation on the systems are summarized in Fig. 2. At first sight, it is clear that calcinations treatments at the highest temperature (850 °C) resulted in the most efficient systems. Moreover, the treatment in a synthetic air flow led to better results as compared to solids submitted to hydrogen (Fig. 2A). Finally, even though Degussa P25 titania was the solid for which glucose disappearance was the fastest (Fig. 2B), it hardly yielded H2 which evidences the role of metals in the process. The discussion on the complex mechanisms of hydrogen formation is beyond the scope of this short communication [14], [15] and [16]. Hereinafter, discussion will be focused on the description of structure-activity relationships in hydrogen generation from glucose aqueous solutions.

Some of the main features concerning characterization of metal-containing system are summarized in Table 1. As can be seen, reduction or oxidation treatment at a temperature significantly higher than 500 °C resulted in a dramatic decrease in surface area, accompanied by a significant increase in the TiO2 crystallite size and its transformation from 100% anatase to 100% rutile (Table 1). Interestingly, reduction of Pd-systems at 850 °C lead to 100% rutile whereas some anatase is present in systems calcined in air flow (7%). XRD diffractograms corresponding to all metal-containing systems are depicted in Fig. 3A and B. Platinum metal phase could be identified in the XRD patterns through its reflections at 2θ = 39.73, 46.24, and 67.41 (Pt metal, JCPDS 4–802) (Fig. 3A). Interestingly, the presence of Pt0 was detected in the system resulting from oxidation at 850 °C but not in the Pt-system calcined at 500 °C nor in the ones obtained after reduction at any temperature (Pt-500-H or Pt-850-H). The formation of Pt0 on oxidation at high temperatures, has already been reported in the literature [17]. From Fig. 3B it is clear that thermal treatments at 850 °C lead to the appearance of palladium crystal phases which is indicative of an increase in particle size. As expected, the system reduced at 850 °C exhibit Pd0 particles at ca. 2θ = 40.0 (111 reflection) [18], [19] and [20]. More interestingly, calcination in synthetic air flow leads to different palladium species. Therefore, both Pd0 (111 reflection at 2θ = 40.08) and PdO (101 reflection at 2θ = 33.98) [21] and [22] can be seen. As shown for platinum systems, the formation of Pd0 under oxidant conditions can be ascribed to the decomposition of palladium oxide into Pd and oxygen which has been reported to occur on calcination at high temperatures [21] and [23].

TEM images of Pt-850-Air, Pt-850-H, Pd-850-Air and Pd-850-H are compared in Fig. 4. Me-850-Air systems are agglomerates of metal particles with a diameter of ca. 50 nm as observed in Fig. 4a and b, whereas smaller and more uniformly distributed metal particles are distinguished in the case of Me-850-H systems (Fig. 4c,d). The greater size of metal (Me) particles in Me-850-Air could explain the detection of peaks of Pt0 and Pd0 in the corresponding XRD.

The determination of the nature and oxidation state of Pt species (Pt0, Pt2+ and Pt4+) and Pd species (Pd0, Pd2+ and Pd4+) is normally accomplished using XPS technique and in particular by means of the study of Pt(4f) and Pd(3d) peaks, respectively (Table 1 and Fig. 5A,B). It is known that metallic Pt0 has binding energies of 70.7–70.9 and 74.0–74.1 eV for 4f7/2 and

4f5/2 electrons, respectively [24] and [25]. In oxidized states, Pt2+ and Pt4+ exhibit much higher binding energies: 72.8–73.1 eV (4f7/2) and 76.3–76.4 eV (4f5/2) for Pt2+ and 74.6–74.9 eV (4f7/2) and 78.1–78.2 eV (4f5/2) for Pt4+[25], [26], [27] and [28]. After reduction in H2/Ar flux at 850 °C (Pt-850-H), two main peaks at 70.4 and 73.8 eV are observed thus indicating the presence of Pt0. However, the values are slightly shifted to lower binding energies as compared to data reported in the literature [24] and [25] (around 0.3 eV, Fig. 5A) which can be indicative of SMSI effect as reported for Pt-CeO2[29] and Pt/TiO2[30] catalysts. Therefore, electrons could be donated from TiO2 to Pt, thus forming (Pt)nσ− species. Under UV irradiation, SMSI effect could avoid electron–hole recombination thus accounting for the improvement in catalytic performance of samples calcined at 850 °C as compared to Pt-500-Air (Fig. 2AB). Moreover, the more pronounced such an effect (case of Pt-850-Air), the better the photocatalytic performance in hydrogen evolution. Examining the chemical composition on the surface from XPS (Table 1), it is worth mentioning that the O/Ti ratios for all samples prepared at 850 °C (except for Pd-850-H, O/Ti ~ 2.09) are slightly below the stoichiometric value. These results allow us to expect a certain number of oxygen vacancies in the systems which additionally can contribute to the decrease of the electron/hole recombination rate by the fact that these vacancies are potential electron traps.

In the case of Pd-systems, it is known that metallic Pd0 has binding energies of 334.9 ± 0.2 eV [31], [32] and [33] while palladium in oxidized states, Pd2+ and Pd4+ exhibits much higher binding energies: 336.4 eV (3d5/2) for Pd2+ and 337.6 eV (3d5/2) for Pd4+ in PdO and PdO2, respectively [22] and [34]. The oxidation treatment in air flux at 850 °C, led to a Pd-XPS profile in which palladium 3d5/2 peaks around 336.4 eV are identified indicating the presence of Pd2+ (probably as PdO) at the catalyst surface. The fact that Pd0 is not detected by XPS but observed through XRD, suggests that such species are present in the bulk of Pd-850-Air. In the case of Pd-850-H the band is slightly shifted to lower binding energy (334.6 eV) (Fig. 5B) which could be ascribed to a greater metal–support interaction [11]. This catalytic system, although having a SMSI effect higher than Pd-850-Air, is less effective in terms of hydrogen production. This observation can be explained by the fact that Pd-850-H exhibits 3.6-fold higher surface Pd/Ti atomic ratio than Pd-850-Air. The recombination rate increases with the metal concentration because the distance between trapping sites in a particle decreases with the amount of metals. Pichat et al. [35] found that there is an optimum metal/ titania ratio below which the metal reduces the charge recombination in TiO2 whereas above such a value recombination at the metal particles progressively cancels such a beneficial effect. Additionally, the high H2 evolution for Pd-850-Air could be related to the O/Ti atomic ratio (O/Ti = 1.90) which is slightly below the stoichiometric value (O/Ti = 2.0), allowing the formation of oxygen vacancies (e− traps) thus decreasing the e−/hole recombination rate.

All in all, the calcination of metal-containing systems resulted in an improvement in photocatalytic efficiency for hydrogen production (Fig. 2A). This is especially significant in the case of Pt-850-Air, Pt-850-H and Pd-850-Air. So much so, that such systems, and the ones prepared at 500 °C, yielded better hydrogen evolution than Degussa P25 (Fig. 2A), the most-widely used photocatalyst. This is particularly remarkable considering that systems prepared at 850 °C consist in very low surface area rutile titania particles. Therefore, such systems should

have exhibited worse catalytic performance than the ones prepared at 500 °C in terms of hydrogen production but we observed quite the opposite. Generally, in terms of glucose disappearance, the ones prepared at 500 °C are more active (Degussa-P25 as the most active) (Fig. 2B) than the ones calcined at 850 °C. Based on our results, we can suggest that the hydrogen production improvement should be associated with the presence of metal (especially for Pt-850-Air with a Pt/Ti atom ratio of 0.8), oxygen vacancies and the proposed SMSI interaction between metal and TiO2.

4. Conclusions

Metals (Pt, Pd) incorporation into the titania surface was favorable for photocatalysis (especially for Pt-systems). Photocatalytic behavior was especially remarkable (increase in hydrogen molar production) in the case of oxidative treatment at 850 °C. XPS analyses showed that systems treated at 850 °C consisted of negatively charged platinum particles (the most active photocatalytic system in this reaction) thus suggesting the electron transfer from TiO2 to Pt (SMSI). Moreover, the greater the SMSI effect, the better the catalytic performance. Such SMSI effect would prevent electron–hole recombination which could explain that, even though oxidation/reduction treatment at 850 °C had led to a decrease in surface area and transformation of anatase to rutile, an improvement in photocatalytic activity was observed. Additionally, it is worthy of mention the importance of the spill-over effect in the surface process of hydrogen production.

All catalysts prepared at 500 °C were less selective for hydrogen production.

The whole process may be described as a photocatalytic reforming of organic wastewater at room temperature and represents an environmentally friendly and cost effective method for water purification with parallel production of energy.

Acknowledgments

References

[1] M.Y. Ni, D.Y.C. Leung, M.K.H. Leung, K. Sumathy

Fuel Processing Technology, 87 (2006), p. 461

[2] S. Rapagna, N. Jand, P.U. Foscolo

International Journal of Hydrogen Energy, 23 (1998), p. 551

[3] W. Iwasaki

International Journal of Hydrogen Energy, 28 (2003), p. 939

[4] S.G. Li, S.P. Xu, S.Q. Liu, C. Yang, Q.H. Lu

Fuel Processing Technology, 85 (2004), p. 1201

[5] M. Watanabe, H. Inomata, K. Arai

Biomass and Bioenergy, 22 (2002), p. 405

[6] X.H. Hao, L.J. Guo, X. Mao, X.M. Zhang, X.J. Chen

International Journal of Hydrogen Energy, 28 (2003), p. 55

[7] M. Ni, M.K.H. Leung, D.Y.C. Leung, K. Sumathy

Renewable & Sustainable Energy Reviews, 11 (2006), p. 401

[8] A. Kudo

International Journal of Hydrogen Energy, 31 (2006), p. 197

[9] A.L. Linsebigler, G.Q. Lu, J.T. Yates

Chemical Reviews, 95 (1995), p. 735

[10] S.J. Tauster, S.C. Fung, R.L. Garten

Journal of the American Chemical Society, 100 (1978), p. 170

[11] M.A. Aramendía, J.C. Colmenares, A. Marinas, J.M. Marinas, J.M. Moreno, J.A. Navío, F.J. Urbano

Catalysis Today, 128 (2007), p. 235

[12] M.A. Aramendía, J.C. Colmenares, A. Marinas, J.M. Marinas, J.A. Navío, F.J. Urbano

Applied Catalysis B: Environmental, 80 (2008), p. 88

[13] J.C. Colmenares, M.A. Aramendia, A. Marinas, J.M. Marinas, F.J. Urbano

Applied Catalysis A: General, 306 (2006), p. 120

[14] X. Fu, J. Long, X. Wang, D.Y.C. Leung, Z. Ding, L. Wu, Z. Zhang, Z. Li, X. Fu

International Journal of Hydrogen Energy, 33 (2008), p. 6484

[15] D.I. Kondarides, V.M. Daskalaki, A. Patsoura, X.E. Verykios

Catalysis Letters, 122 (2008), p. 26

[16] H. Bahruji, M. Bowker, P.R. Davies, L.S. Al-Mazroai, A. Dickinson, J. Greaves, D. James, L. Millard, F. Pedrono

Journal of Photochemistry and Photobiology A: Chemistry, 216 (2010), p. 115

[17] C.P. Hwang, C.T. Yeh

Journal of Molecular Catalysis A: Chemical, 112 (1996), p. 295

[18] K.I. Shimizu, S. Koizumi, T. Hatamachi, H. Yoshida, S. Komai, T. Kodama, Y. Kitayama

Journal of Catalysis, 228 (2004), p. 141

[19] N. Macleod, J.M. Keel, R.M. Lambert

Applied Catalysis A: General, 261 (2004), p. 37

[20] V.N. Kalevaru, A. Benhmid, J. Radnik, M.M. Pohl, U. Bentrup, A. Martin

Journal of Catalysis, 246 (2007), p. 399

[21] W. Lin, L. Lin, Y.X. Zhu, Y.C. Xie, K. Scheurell, E. Kemnitz

Journal of Molecular Catalysis A: Chemical, 226 (2005), p. 263

[22] Y. Bi, G. Lu

Applied Catalysis B: Environmental, 41 (2003), p. 279

[23] C.B. Wang, H.G. Lee, T.F. Yeh, S.N. Hsu, K.S. Chu

Thermochimica Acta, 401 (2003), p. 209

[24] T. Teranishi, M. Hosoe, T. Tanaka, M. Miyake

The Journal of Physical Chemistry. B, 103 (1999), p. 3818

[25] Y. Nagai, H. Shinjoh, K. Yokota

Applied Catalysis B: Environmental, 39 (2002), p. 149

[26] T. Wang, A. Vazquez, A. Kato, L.D. Schmidt

Journal of Catalysis, 78 (1982), p. 306

[27] V. Romanovskaya, M. Ivanovskaya, P. Bogdanov

Sensors and Actuators B: Chemical, 56 (1999), p. 31

[28] S. Zafeiratos, G. Papakonstantinou, M.M. Jacksic, S.G. Neophytides

Journal of Catalysis, 232 (2005), p. 127

[29] M. Abid, V. Paul-Boncour, R. Touroude

Applied Catalysis A: General, 297 (2006), p. 48

[30] H. Lida, A. Igarashi

Applied Catalysis A: General, 303 (2006), p. 192

[31] V.V. Kaichev, M. Morkel, H. Unterhalt, I.P. Prosvirin, V.I. Bukhtiyarov, G. Rupprechter, H.J. Freund

Surface Science, 566–568 (Pt. 2) (2004), p. 1024

[32] A.S. Mamede, G. Leclercq, E. Payen, P. Granger, L. Gengembre, J. Grimblot

Surface and Interface Analysis, 34 (2002), p. 105

[33] O. Demoulin, M. Navez, P. Ruiz

Catalysis Letters, 103 (2005), p. 149

[34] G. Ketteler, D.F. Ogletree, H. Bluhm, H. Liu, E.L.D. Hebenstreit, M. Salmeron

Journal of the American Chemical Society, 127 (2005), p. 18269

[35] P. Pichat, J.M. Herrmann, J. Disdier, M.N. Mozzanega, H. Courbon

Studies in Surface Science and Catalysis, 19 (1984), p. 319

Figure captions

Figure 1. Synthetic methodology for the systems used as photocatalysts in the present work.

Figure 2. Results obtained for photocatalytic experiments on the different systems expressed in terms of hydrogen formation (A) and glucose disappearance (B).

Figure 3. X-Ray diffractograms of the solids.

Figure 4. TEM micrographs of Pt-850-AIR (A), Pd-850-AIR (B), Pt-850-H (C) and Pd-850-H (D).

Figure 5. Pt 4f (A) and Pd 3d (B) XPS spectra of the systems calcined at 850 °C.

Table 1

Table 1. Summary of the most remarkable features concerning characterization of Me/TiO_2 system (where, Me = Pt or Pd).

Photocatalyst	XRD		N_2 ISOTHERMS	XPS	
	Crystal phases[a] (%)	Crystallite size (nm)	S_{BET} (m²/g)	Me/Ti atomic %	O/Ti
Pt-500-Air	100%A	21	57	—[b]	1.86
Pt-500-H	100%A	23	50	not determined	
Pt-850-H	100%R	77	6	3.50	1.92
Pt-850-Air	100%R + Pt^0	66	6	0.88	1.92
Pd-500-Air	100%A	18	75	0.91	1.75
Pd-500-H	100%A	21	62	0.85	1.95
Pd-850-H	100%R + Pd^0	81	5	3.12	2.09
Pd-850-Air	93%R, 7%A + PdO + Pd^0	116(R), 66(A)	7	0.87	1.90

a A and R denote anatase and rutile, respectively.
b Quantification of platinum at.% present at the surface of Pt-500-Air was not possible since the intensity of Pt(4f) peak was very small.
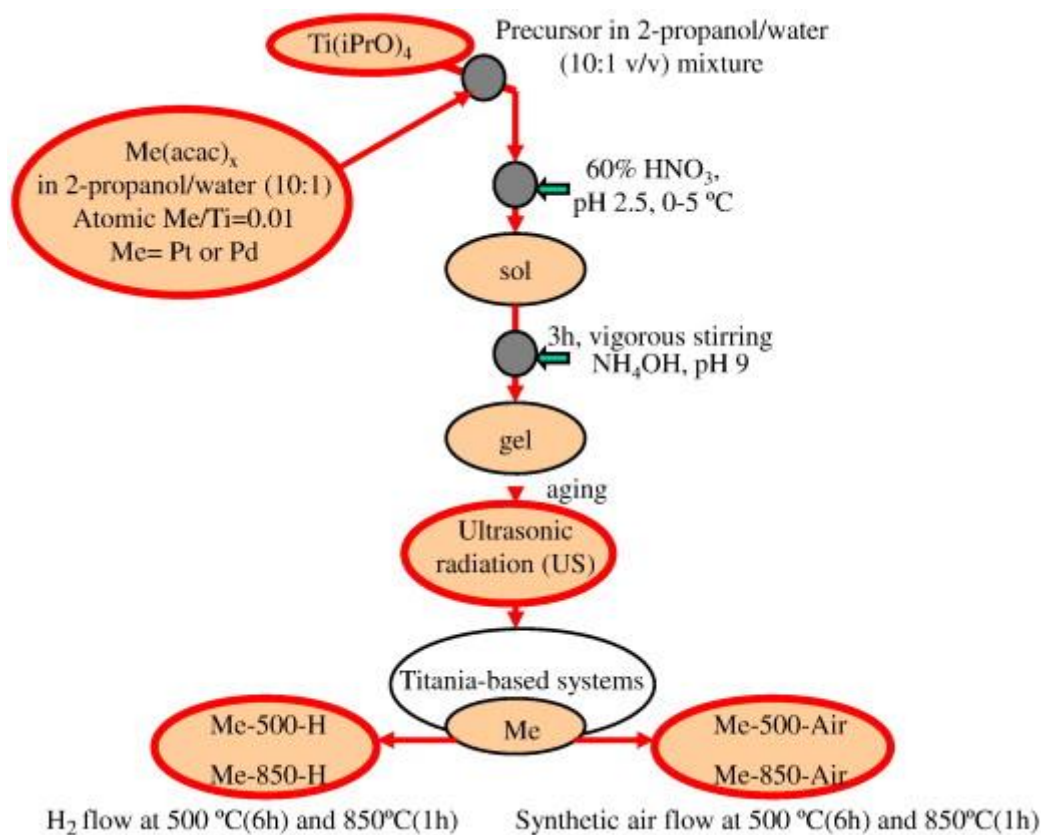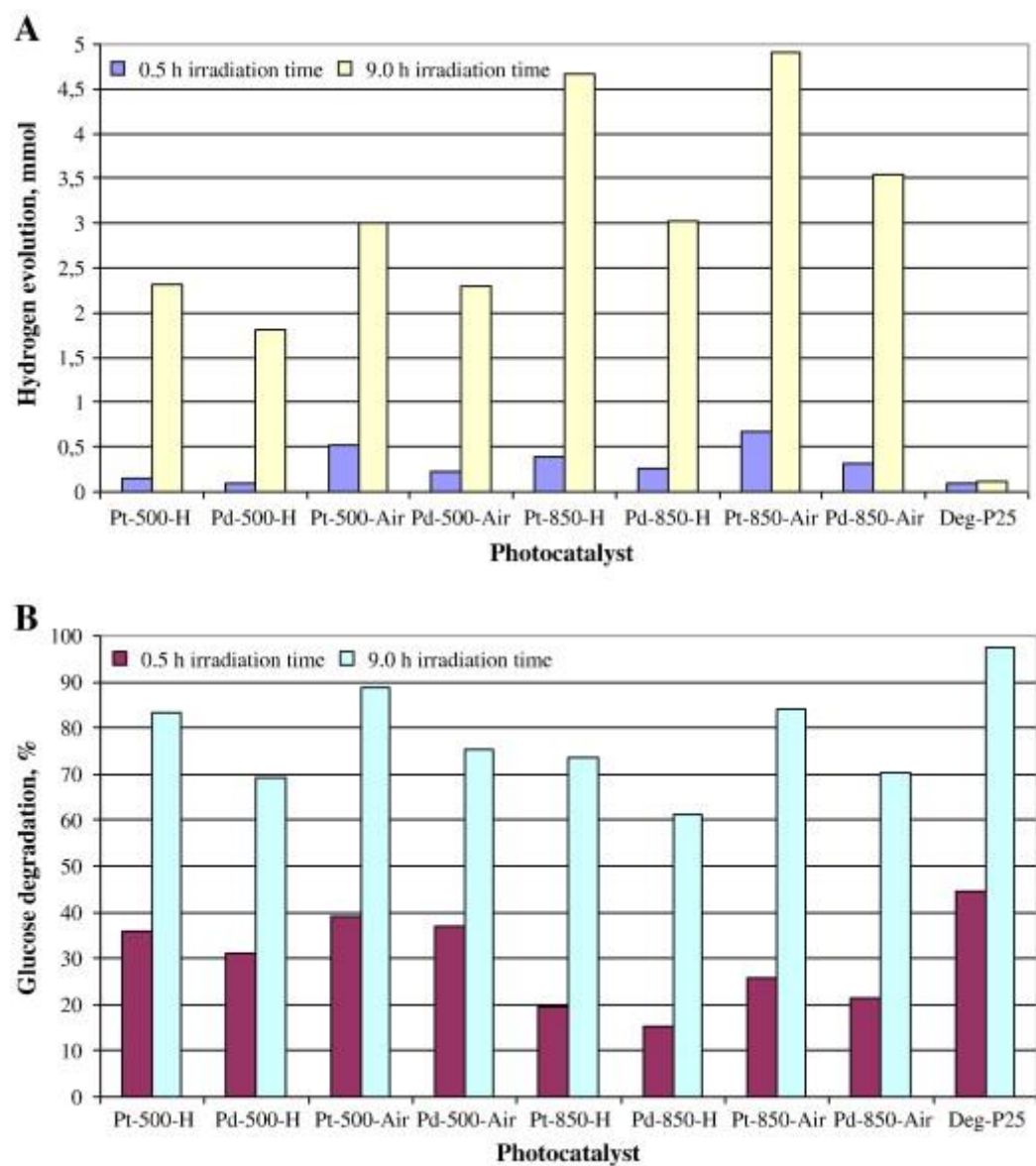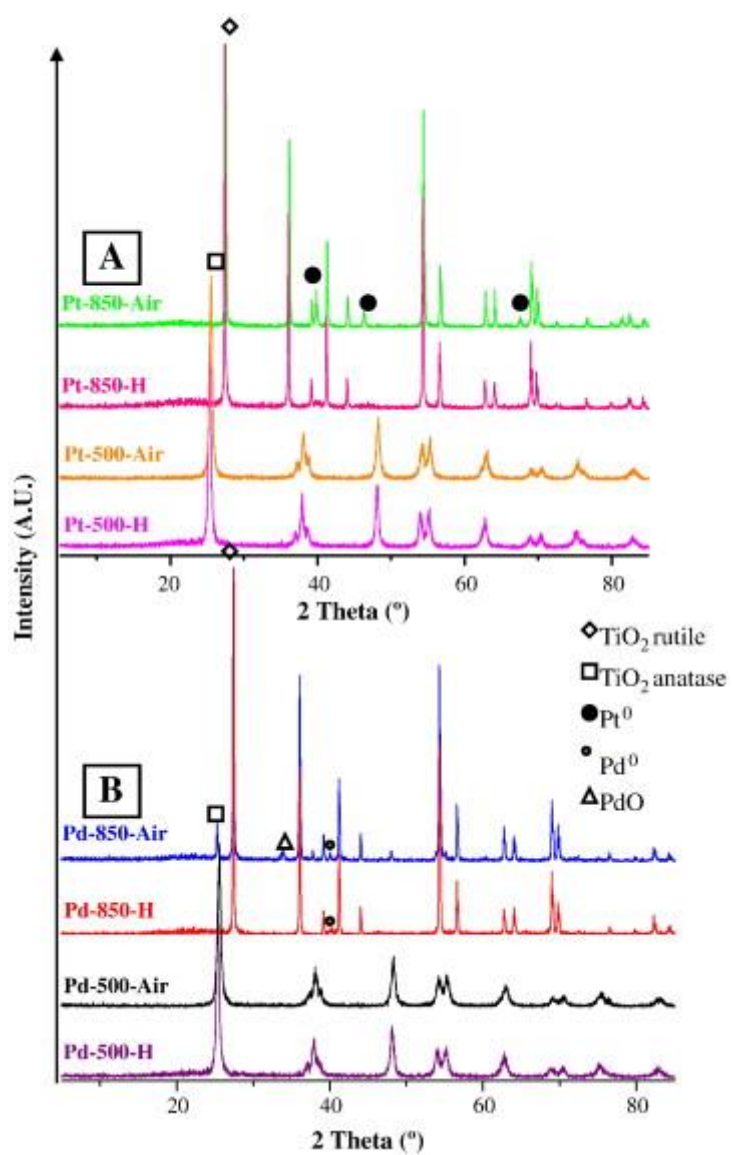
Figure 1

Figure 2

Figure 3

Figure 4

Figure 5